applied sciences

MDPI

Article

Estimation of Soil Shear Strength Indicators Using Soil Physical Properties of Paddy Soils in the Plastic State

Qianjing Jiang, Ming Cao, Yongwei Wang *, Jun Wang and Zhuoliang He

Department of Biosystems Engineering, Zhejiang University, 866 Yuhangtang Road, Hangzhou 310058, China; jqj713@zju.edu.cn (Q.J.); 21613004@zju.edu.cn (M.C.); jwang@zju.edu.cn (J.W.); zhuolianghe@zju.edu.cn (Z.H.)
* Correspondence: wywzju@zju.edu.cn

Abstract: Saturated soil shear strength is a primary factor that reflects the driving resistance of agricultural machinery in paddy soils. The determination of soil shear strength indicators, such as cohesion and internal frictional angle, is crucial to improve the walking efficiency of agricultural machinery in paddy soils. However, the measurement of these indicators is often costly and time-consuming. Soil moisture content, density, and clay content are crucial factors that affect the cohesion and internal friction angle, while very limited studies have been performed to assess the interactive effects of the three factors on soil shear characteristics, especially on paddy soils. In this study, eight soil samples were taken from eight paddy fields in Southeastern China, and the central composition rotatable design was used to classify the soil samples into five levels based on different clay content (X_1), moisture content (X_2), and density (X_3). The direct shear tests were carried out indoors on the remolded paddy soil using a self-made shear characteristic measuring device. Then, both individual and interactive effects of X_1, X_2, and X_3 on soil cohesion and internal friction angles on paddy soils were systematically investigated and analyzed using the regression analysis method in the data processing software Design-Expert. Our results indicated that the effects of the three environmental factors on soil cohesion were in the order of $X_1 > X_2 > X_3$, while the order was $X_2 > X_3 > X_1$ for the impact on internal friction angle. The interactive effects were in the order of $X_1X_2 > X_1X_3 > X_2X_3$ for cohesion and $X_1X_2 > X_2X_3 > X_1X_3$ for internal friction angle. Two prediction models were successfully established to quantify the soil cohesion and internal friction angle as affected by soil physical properties, and the coefficient of determination (R_2) was 0.91 and 0.89 for the two equations, respectively. The model validations using new soil samples suggested that the models were capable of predicting the shear characteristic parameters under different physical parameters effectively, with errors between predicted and measured soil shear strength indicators within 15% and relative root mean square error less than 11%.

Keywords: shear strength; cohesion; internal friction angle; moisture content; density; clay content

Citation: Jiang, Q.; Cao, M.; Wang, Y.; Wang, J.; He, Z. Estimation of Soil Shear Strength Indicators Using Soil Physical Properties of Paddy Soils in the Plastic State. *Appl. Sci.* **2021**, *11*, 5609. https://doi.org/10.3390/app11125609

Academic Editor: Itzhak Katra

Received: 30 April 2021
Accepted: 15 June 2021
Published: 17 June 2021

1. Introduction

Rice (*Oryza sativa* L.) is an important grain crop that ranks second only to wheat as the most extensively grown crop in the world, feeding more than 50% of the world's population [1,2]. As a paddy field grown crop, the total area of paddy fields in China has contributed to 29% of the world's total rice cultivation area [3]. The production of rice is highly dependent on the efficiency of the walking performance of agricultural machinery; however, the difficulties of agricultural machinery for walking in the narrow and muddy paddy fields due to soil resistance have restricted the agronomic management practices during rice planting [4]. Therefore, it is crucial to understand the factors that affect soil physical characteristics when designing agricultural machinery, thereby reducing the driving resistance and improving the walking performance in paddy fields.

The dynamics of soil shear strength are essential to understand the mechanic behavior of agricultural soils [5], which would affect the driving resistance of agricultural machinery [6,7]. The interaction between soil and machinery results in soil shear damage and

thereby produces walking resistance [8]. Soil shear strength is reflected from two factors: the physicochemical bonds (cohesion) and internal frictional resistance (determined by the internal friction angle) between particles [9,10]. Therefore, the cohesion and internal friction angle have been extensively investigated to characterize soil shear properties [11,12].

The determination of soil shear strength through lab measurements is costly and time-consuming; therefore, efforts have been undertaken to study the relationships between different soil properties and soil shear strength [13]. Soil moisture content has been extensively reported as a significant contributor to soil shear strength due to its impact on cohesion and internal friction strength [14–20], while their relationship remained controversial across soil types and locations. In addition to soil moisture content, other soil physical parameters that affect the soil shear strength have been reported, including soil texture [18,21], density [14,15,17,21–23], particle size distribution [24], soil particle properties and boundary conditions [25], vegetation and plant roots [26,27], and shear loading [19,28]. Some researchers also suggested that soil shear strength would be affected by soil organic matter content through its impact on bulk density or cohesive forces between the soil particles [13,29–31]. It is very difficult to take the measurements of all the influencing environmental factors and quantify their impact on soil cohesion strength [23]; therefore, it is necessary to select the most important factors. The current study focused on three soil physical properties that are quick and easy to measure, including soil moisture content, clay content, and density.

To date, most of the published works have been carried out on upland soils with low moisture content or the rheology of paddy soils with high moisture content, while the shear characteristics of paddy soil in the plastic state have rarely been studied. Furthermore, these studies mostly focused on single or two soil physical parameters as influencing factors, while there is limited research on the quantitative relationships between shear strength indicators with soil moisture, density, and texture. Therefore, the objectives of this paper were (1) to assess the impact of different soil physical parameters on shear strength characteristics of paddy soils in plastic condition; and (2) to establish a prediction model for estimating the cohesion and internal friction angle at a given soil clay content, moisture content and density.

2. Materials and Methods

The experiments of this study were carried out in the Department of Biosystem Engineering in Zhejiang University, Hangzhou, China.

2.1. Soil Collection and Preparation

The Yangtze River Delta is one of the most traditional rice-growing regions in Southeastern China. Soil samples were taken from eight different paddy fields in the provinces of Zhejiang, Jiangsu, and Anhui within this region, while measured soil physical properties, including fractions of sand, silt, and clay, soil texture, plastic limit, liquid limit, and plasticity index, are shown in Table 1.

Table 1. Measured soil physical properties.

Sample No.	Sample Location	Sand (%)	Silt (%)	Clay (%)	Soil Texture	Plastic Limit (%)	Liquid Limit (%)	Plasticity Index (%)
1	Huzhou, Zhejiang	1.6	57.8	40.6	Silty clay	22.0	49.5	27.5
2	Shaoxing, Zhejiang	27.9	49.8	22.3	Loam	24.0	51.8	27.8
3	Hangzhou, Zhejiang	1.8	68.9	29.3	Silty clay loam	30.3	52.5	22.2
4	Wuhu, Anhui	11.3	62.6	26.1	Silty clay loam	23.5	49.0	25.5
5	Yixing, Jiangsu	4.0	60.0	36.0	Silty loam	31.5	52.5	21.0
6	Hangzhou, Zhejiang	15.4	61.1	23.5	Silty clay loam	18.5	61.5	43.0
7	Huzhou, Zhejiang	5.5	63.7	30.8	Silty clay loam	23.5	49	25.5
8	Nanjing, Jiangsu	3.5	73.7	22.8	Silty loam	18.5	55.5	37.0

2.2. Theory of Soil Shear Strength

Soil shear strength reflects the maximum shear stress that a soil can sustain [10]. The shear strength for saturated soil is determined from the Mohr–Coulomb failure equation [32] as follows:

$$\tau = \sigma \cdot \tan \varphi + c \quad (1)$$

where τ (kPa) is the shear strength, c (kPa) is cohesion, σ is the vertical stress and φ (°) is the angle of internal friction. The soil cohesion and internal friction were measured from the direct shear test, which reflects the cohesive strength of the soil and the friction strength between the soil particles, respectively.

2.3. Experimental Design

To analyze the single and interactive impact of three soil physical parameters, clay content, soil moisture content, and soil wet bulk density, on the cohesion and internal friction angle, the central composition rotatable design was applied to assign individual variables into multiple evaluations [33]. The eight soil samples were classified into five levels (Table 2) and a combination of 20 experimental schemes was therefore scheduled. The zero-horizontal clay content, moisture content and soil wet bulk density were 40%, 30.8%, and 2.3 g cm^{-3}, respectively.

Table 2. Coded levels for different factors.

No.	Code	Coded Levels of Variables		
		Clay Content/%	Moisture Content/%	Wet Bulk Density/g·cm^{-3}
1	−1.682	22.3	30	1.8
2	−1	26.1	34	2.0
3	0	30.8	40	2.3
4	1	36.0	46	2.6
5	1.682	40.6	50	2.8

To obtain the 20 combinations of soil samples with the targeted soil moisture, clay content, and density, as shown in Table 2, the soil samples were remolded according to the National Standard of the People's Republic of China (GB/T50123-1999). Five soil samples which met the requirement of clay content in Table 2 were firstly selected, then water was added into the five samples until moisture content reached the specific values. The completely mixed soils were placed in sealed bags for 6 hours. Subsequently, the soil samples with specific density were modulated by the annular soil collector using the formula below:

$$m = V \cdot \rho \quad (2)$$

where m is the weight of the soil sample which should be added to the soil collector (g), V is the volume of the soil collector (cm^3), and ρ is the specific density as needed (g cm^{-3}). Finally, the target soil samples inside the annular soil collector with specific clay content, moisture content and density were obtained. The remolded soil samples were all stored in sealed bags for another 24 h before the shear strength tests.

2.4. Direct Shear Strength Measurement

Direct shear tests were conducted at Zhejiang University on 3 June 2017 to measure the soil shear strength parameters using a self-made device (Figure 1). After calibrating the instrument, the soil samples in the annular soil collector were placed into the shear box, and the pressure of the cylinder was adjusted using the pressure-regulating valve. When the pressure met the requirement of the experimental setting, the reversing valve was opened and the air was filled in. Subsequently, the shear box was vertically compressed by the cylinder piston and the normal stress was loaded. After that, the mechanical test machine started moving upward at the speed of 0.08 mm min^{-1}, which pulled the wire rope and

thus moved the shear box down. Consequently, one direct shear test was completed when the shear displacement reached 4 mm, and the data of displacement as well as tension were recorded automatically.

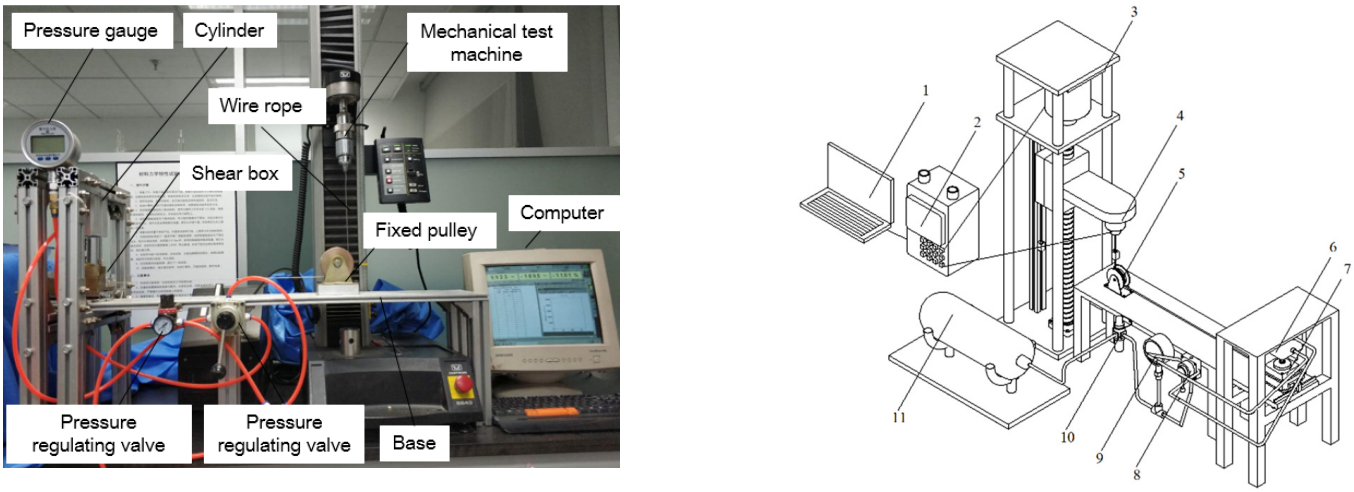

Figure 1. Self-made device for measuring shear characteristics. Note: 1. Computer; 2. Controller; 3. Mechanical test machine; 4. Force sensor; 5. Pulley; 6. Cylinder; 7. Shear box; 8. Gas circuit switch; 9. Pressure gauge; 10. Pressure regulating valve; 11. Air compression machine.

The shear tests for all 20 soil samples were performed with three replications under six different normal stresses, including 25, 50, 67, 83, 100, and 133 kPa, respectively. In total, 360 direct shear tests (20 coded levels × 3 replicates × 6 normal stresses) were performed. After all the tests were completed, the moisture content was measured again to ensure all soil samples were tested under the specific moisture content.

During each direct shear test, when the shear displacement was 4 mm, the maximum force was taken as the maximum shear force of the soil sample under a certain vertical load, and the formula of the shear strength was as follows:

$$\tau = \frac{F_{max}}{s} \tag{3}$$

where τ is the shear strength, F_{max} is the maximum shear force and s is the shear area.

For each soil sample, the vertical stress and shear strength were drawn in the transverse and longitudinal coordinates, and the curves were fitted with a straight line. The angle of the straight line was the internal friction angle, while the intercept of the straight line in the longitudinal coordinates was the cohesion c.

2.5. Data Processing and Statistical Analyses

The response surface methodology was applied to present the response of shear strength indicators to the changes in soil physical properties using quadratic polynomial regression equations. The results from lab experiments were processed and analyzed using the software Design-Expert. The indexes of cohesion (Y_1) and internal friction angle (Y_2) were taken as response values, while soil clay content (X_1), soil moisture content (X_2), and soil wet bulk density (X_3) were set as impacting factors. The relationship between these variables could be represented by a quadratic polynomial regression formula as below:

$$Y = \beta_0 + \beta_1 X_1 + \beta_2 X_2 + \beta_3 X_3 + \beta_{12} X_1 X_2 + \beta_{13} X_1 X_3 + \beta_{23} X_2 X_3 + \beta_{11} X_1^2 + \beta_{22} X_2^2 + \beta_{33} X_3^2 \tag{4}$$

where Y is the response value, X_1, X_2, and X_3 are independent variable encoding values, while β_0, β_1, β_2, β_3, β_{12}, β_{13}, β_{23}, β_{11}, β_{22}, and β_{33} are the regression coefficients of the prediction model.

To establish the effective regression equation to describe the relationship between the response values of soil shear characteristics (cohesion, internal friction angle) and soil physical properties (clay content, moisture content, and density), the analysis of variance (ANOVA) test for all the coefficients was performed using Design-Expert, and the parameters without statistical significance ($p \geq 0.05$) were deleted. Meanwhile, the adequacy of the regression model was assessed by the determination coefficient (R^2). Once the quadratic equations were determined, the 3-D response surface plots were presented to show the interactive effects of the three soil properties on soil cohesion and internal friction angle.

Once the regression coefficients of the prediction model were determined, the accuracy of the model was validated using other soil samples, which were obtained from the 8 original soils using the same treatment as the 20 soil samples in the model setup. Accordingly, the cohesion and internal frictional angle for these soil samples were measured and compared with the estimated values from the prediction model. Finally, the performance of the model was validated with the percent of bias (PBIAS) for each sample and the root mean square error (RMSE) and relative RMSE (RRMSE).

3. Results

3.1. Experimental Results

Table 3 shows the experiment design and results, and the statistical analysis results are shown in Table 4. For the statistical analysis of cohesion (Y_1), the p-value and the coefficient of determination (R_2) were 0.0001 and 0.91, respectively, indicating that the regression model was extremely significant and had high fitting accuracy. In the same way, the statistical analysis of the internal friction angle shows that the p-value and the determining coefficient (R^2) of the total model were 0.0001 and 0.89, respectively. Consequently, the cohesion (Y_1) and internal friction angle (Y_2) can be expressed using the regression equations as follows:

$$Y_1 = 16.22 + 7.04X_1 - 1.51X_2 + 2.77X_1^2 - 1.49{X_3}^2 \quad (5)$$

$$Y_2 = 35.7 - 9.34X_2 - 5.9X_1^2 - 6.27X_2^2 - 5.75{X_3}^2 \quad (6)$$

Table 3. Experiment scheme and test results.

Sample No.	X_1	X_2	X_3	Y_1/kPa	Y_2/°
1	−1	−1	−1	12.81	31.0
2	1	−1	−1	28.64	22.1
3	−1	1	−1	10.37	10.3
4	1	1	−1	24.26	2.8
5	−1	−1	1	13.64	35.2
6	1	−1	1	28.77	25.3
7	−1	1	.1	8.37	15.0
8	1	1	1	23.63	6.1
9	−1.682	0	0	11.21	14.0
10	1.682	0	0	32.65	22.1
11	0	−1.682	0	14.57	31.3
12	0	1.682	0	12.57	2.7
13	0	0	−1.682	6.83	24.3
14	0	0	1.682	12.98	12.6
15	0	0	0	17.57	34.41
16	0	0	0	15.24	34.57
17	0	0	0	16.37	38.03
18	0	0	0	15.12	37.42
19	0	0	0	16.4	34.14
20	0	0	0	17.36	35.98

Table 4. Variance analysis of factors to cohesion and internal friction angle.

Coefficient	Y_1 (Cohesion)			Y_2 (Internal Friction Angle)		
	Value	F Value	*p* Value	Value	F Value	*p* Value
β_0	16.22			35.7		
β_1	7.04	88.17	<0.0001	−1.58	−5.75	0.2960
β_2	−1.51	4.04	0.0721	−9.34	42.45	<0.0001
β_3	0.64	0.72	0.4169	−0.31	0.048	0.8314
β_{12}	−0.23	0.053	0.8220	0.30	0.026	0.8759
β_{13}	0.084	0.01	0.9336	−0.30	0.026	0.8759
β_{23}	−0.45	0.21	0.6567	0.075	0.001	0.9688
β_{11}	2.77	14.36	0.0035	−5.90	17.86	0.0018
β_{22}	−0.19	0.067	0.8007	−6.27	20.18	0.0012
β_{33}	−1.49	4.14	0.0693	−5.75	17.02	0.0021
p value		<0.0001			<0.0001	
R^2		0.91			0.89	

3.2. Analysis of Single Factors

The effect of the single factor on the response value was analyzed by the dimensionality reduction method. In the regression equation of the response value, other factors were fixed at zero levels, and the curves of the single factor and response value for the cohesion and internal friction angle are shown in Figure 2. According to the analysis in Table 4 and Figure 2, soil cohesion decreased with the increase in soil moisture content and increased with higher clay content. However, it increased slightly at first but then decreased when wet bulk density reached 2.3 g cm^{-3}. Among the three factors, clay content had the greatest impact on cohesion with the largest slope of the regression line. The internal friction angle showed similar responses to the changes in clay content, moisture content and wet bulk density, which all increased until the three factors reached the central level and then dropped when the factors continued increasing. Soil moisture content was the primary factor that affected the internal friction angle among the three factors.

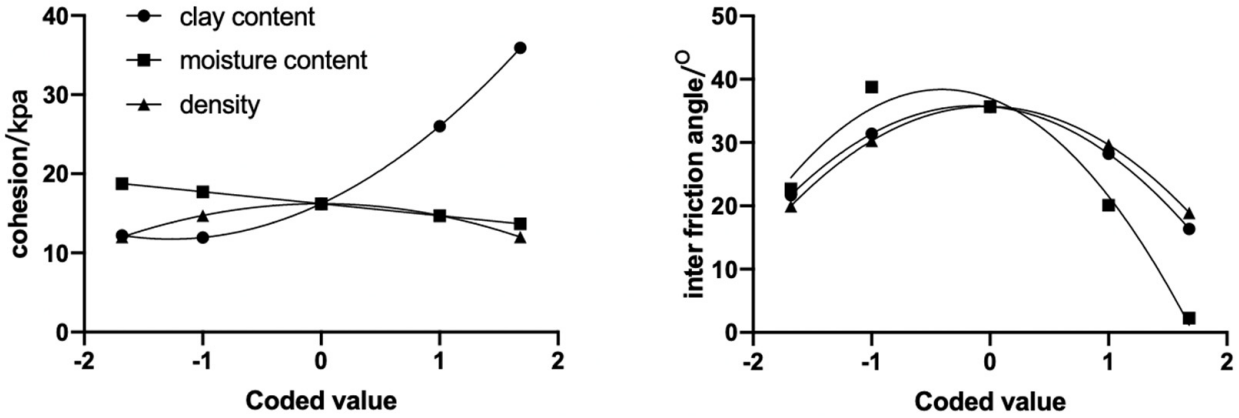

Figure 2. Single-factor effect curves.

3.3. Analysis of Interactive Factors

Two interactive factors of clay content, water moisture content, and density on soil shear strength were analyzed, with the response surface of soil cohesion and internal friction angle to these factors shown in Figures 3 and 4.

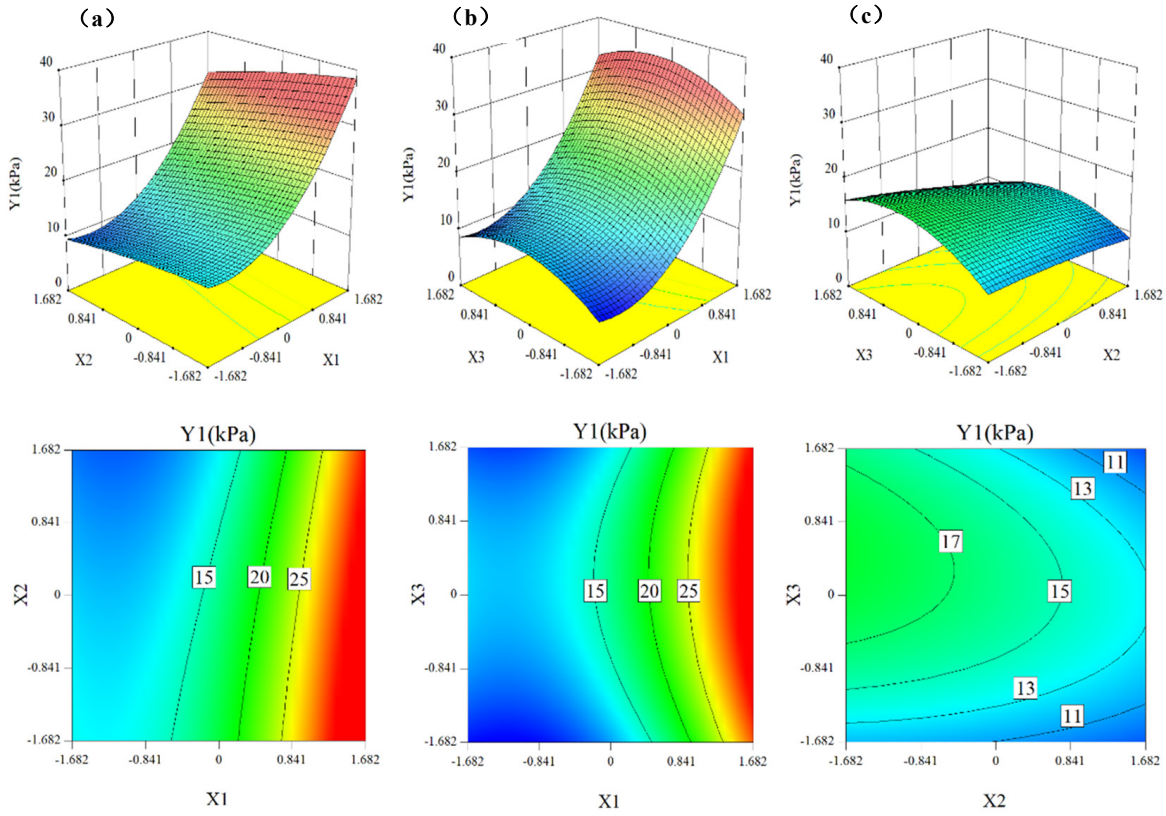

Figure 3. Interactive effects of (**a**) clay content and moisture content; (**b**) clay content and soil wet bulk density; (**c**) moisture content and soil wet bulk density on cohesion.

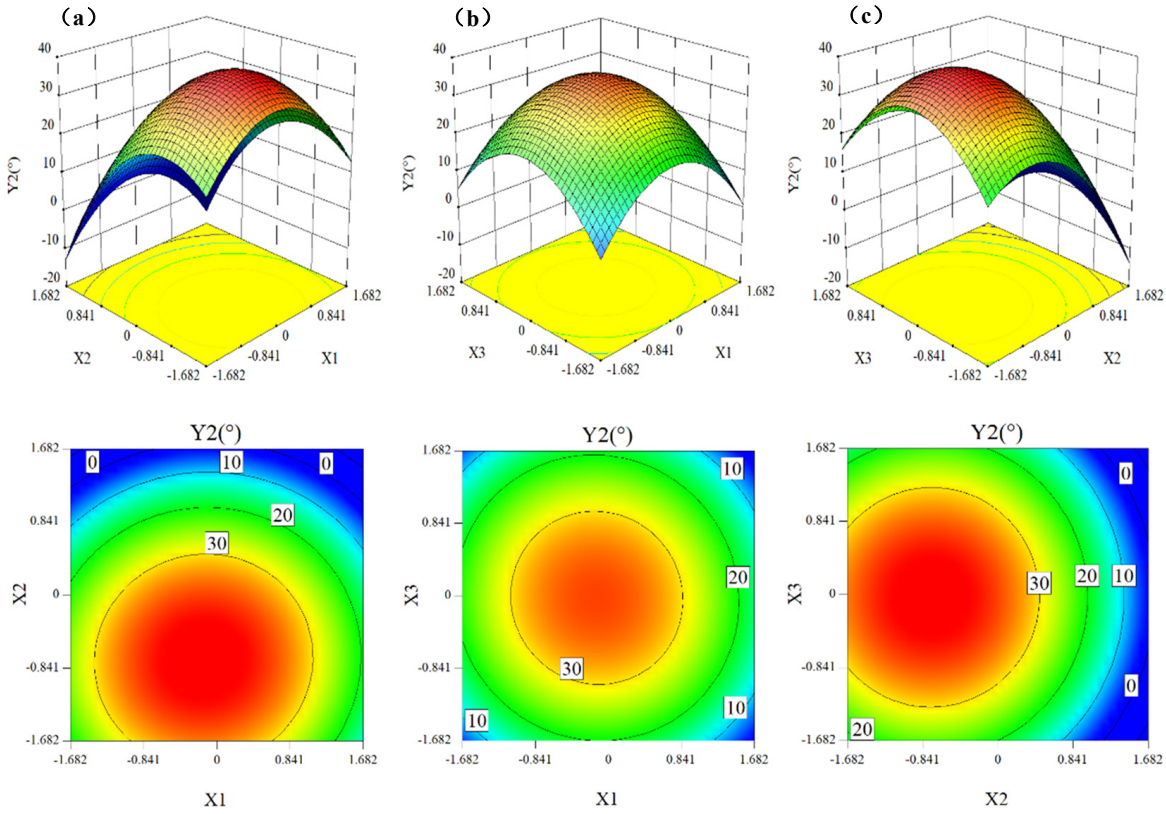

Figure 4. Interactive effects of (**a**) clay content and moisture content; (**b**) clay content and soil wet bulk density; (**c**) moisture content and soil wet bulk density on internal friction angle.

3.3.1. Analysis of Interactive Factors on Cohesion

When the soil wet bulk density was 2.3 g cm^{-3}, the cohesion increased with the increase in clay content and moisture content (Figure 3a). The maximum soil cohesion value was obtained when clay content was within 36–40% (the coded value within 1–1.682) and moisture content within 30–34% (the coded value within −1.682–1). The contour map showed that the variation rate of cohesion along the direction of clay content was higher than that of moisture content, which indicated a greater influence of clay content on soil cohesion than moisture content. In Figure 3b, when the moisture content was 40%, cohesion increased firstly and then decreased with the increase in clay content and density. The maximum cohesion was reached when clay content was between 36 and 40% (coded value 1–1.682) and density was between 2.6 and 2.8 g·cm^{-3} (coded value 1–1.682). The contour map suggests a greater impact of clay content on soil cohesion than moisture content, as the variation rate of cohesion along the direction of clay content was greater than density. Figure 3c shows that cohesion decreased with the increase in moisture content and density when the clay content was 31%. The highest cohesion was estimated when the moisture content and density were within 30~34% (coded value −1.682~−1) and 2.6~2.8 g·cm^{-3} (coded value 1~1.682), respectively. Moreover, as shown from the various rates of cohesion in different directions in Figure 3c, the soil moisture content has a greater impact on cohesion than wet bulk density. However, the interactive effect of these two factors on cohesion was negligible ($p > 0.1$).

To summarize, the contribution rates of clay content (X_1), moisture content (X_2), and density (X_3) to cohesion from high to low followed the order $X_1 > X_2 > X_3$ (Table 5). Considering the interactive influences of two factors on soil cohesion, the contribution rates from high to low were ordered as $X_1X_2 > X_1X_3 > X_2X_3$.

Table 5. The measured and predicted values of the shear parameters model.

No.	Clay/%	Moisture/%	Density/	Cohesion/kPa		Friction Angle/°	
			g·cm^{-3}	MV	PV	MV	PV
1	22.3	35	2.1	11.3	11.9	22.6	22.2
2	22.8	40	2.6	17.5	11.1	32.6	26.7
3	23.5	40	2.0	15.2	9.9	23.9	19.3
4	26.1	40	2.0	10.7	10.0	20	26.2
5	30.8	35	2.3	21.6	17.3	30.2	39.1
6	30.8	40	2.6	28.3	15.2	10.3	9.3
7	36.0	35	2.3	25.3	28.0	30.2	30.7
8	36.0	40	2.6	21.3	25.9	14.3	21.2
Average				18.9	16.2	20.0	24.3
PBIAS				15%		−6%	
RMSE				2.05		1.94	
RRMSE				11%		8%	

MV: measured value; PV: predicted value; PBIAS: percent of bias; RMSE: root mean square error; RRMSE: relative root mean square error.

3.3.2. Analysis of Interactive Factors on Internal Friction Angle

The interactive impact of two factors on internal friction angle is shown in the contour maps in Figure 4. As illustrated by Figure 4a, the internal friction angle decreased with the increase in clay content and moisture content when the soil density was 2.3 g cm^{-3}. Similar to cohesion, the maximum internal friction angle was obtained when clay content was within 36–40% (the coded value within 1–1.682) and moisture content within 30–34% (the coded value within −1.682–1). However, the contour map suggested that the moisture content has a greater impact on the internal friction angle than clay content, which was opposite to their effects on cohesion, as discussed in Section 3.3.1.

When the moisture content was kept constant at the value of 40%, the internal friction angle increased with both the clay content and density, as shown in Figure 4b. The

maximum internal friction angle was reached when clay content was between 36 and 40% (coded value 1–1.682) and density was between 2.6 and 2.8 g·cm^{-3} (coded value 1–1.682). Meanwhile, as compared to clay content, the wet bulk density had a greater impact on internal friction angle.

Figure 4c implies that the internal friction angle decreased with the increase in moisture content and density when the clay content was 31%. The maximum internal friction angle was obtained when the moisture content and density were within 30~34% (coded value −1.682~−1) and 2.6~2.8 g·cm^{-3} (coded value 1~1.682), respectively. Moreover, the variation rates of the internal friction angle in different directions suggest that the soil moisture content has a greater impact on the internal friction angle than density.

Table 4 shows that the contribution rates of individual factors to the internal friction angle from high to low were X_1, X_2, and X_3 in turn, while the impact of two interactive factors on the internal friction angle from high to low was ordered X_1X_2, X_2X_3 and X_1X_3. However, all three combinations of the interactive impact on the internal friction angle were non-significant ($p > 0.1$).

3.4. Model Validation

To verify the accuracy of the correlation model established in this study, three soil samples with different clay contents, moisture contents, and densities that were not used in the model setup were applied to validate the model. The computed cohesion and internal friction angle were compared to the measured values from direct shear tests (Table 5). The PBIASs between the averaged predicted and measured cohesion and internal friction angle were both within 15%, and the RRMSEs were less than 11%, indicating satisfactory estimations of the soil shear strength indicators.

4. Discussion

Our results show that soil cohesion decreased with the increase in soil moisture content and increased with higher clay content and soil density, which is supported by [34], who found a strong positive correlation between soil cohesion and clay content. Similarly, [19] also demonstrated that soil cohesion increased with clay content. Higher soil wet bulk density resulted in smaller gaps between the soil particles, thereby leading to a larger internal friction angle as well as greater soil cohesion. Many published works suggested that the shear strength increased with water content but decreased when maximum shear strength was reached at a particular water content [18,35]. Ref. [18] suggested a quadratic polynomial relationship between soil cohesion and soil water content ($R^2 > 0.75$, $p < 0.05$), with the maximum cohesion reached when the soil water content was between 14 and 21%. In the current study, the moisture contents of our paddy soil samples were within 22–40%, thus the soil cohesion decreased with increasing soil water content. The effect of moisture content on cohesion was mainly caused by the water film bonding force. With the increase in moisture content, the distance between soil particles and the thickness of the water film increased, and as a result, cohesion between soil particles decreased. Our finding was in order with [20], who indicated a negative impact of soil moisture content on cohesion.

The internal friction angle mainly reflected the friction characteristics between the soil particles, including the sliding friction caused by the roughness of the particle surface, and the biting friction produced by the movement of the particles. Although [19] suggested that soil friction was poorly associated with soil water content and bulk density, our study indicated that soil moisture content played a vital role in the friction angle, as shown in Table 4 and Figure 2. The internal friction angle increased quickly when moisture content increased from 30% to 34%, but then rapidly dropped when it increased from 34% to 50% because lower soil moisture content led to a reduction in the thickness of the water film between soil particles, which means that the gaps between the particles were filled and the inner friction angle became larger. When the soil moisture content exceeded the liquid limit, the inner friction angle would be reduced to zero. As at this time paddy soil would be in a rheological state and the gaps between particles were filled with water, the particles could

move freely without resistance [36]. Our results are supported by [20], who also showed experimental evidence that the internal friction angles decreased with increasing soil water content. Similarly, our study indicated that the internal friction angle both increased at first to the maximum value and then dropped when wet soil bulk density kept increasing. The internal friction angle in paddy soils increased with clay content when it was less than 30%, which is in order with [34], who found fine clays decreased frictional strength greatly in the calcareous soils of central Iran. However, the internal friction angle started to decrease when the clay content continued increasing, which is supported by [37], who reported lower internal friction angles for clayed soils than sandy soils.

5. Conclusions

The current study comprehensively assessed both the individual and interactive impact of three soil physical parameters, including clay content (X_1), moisture content (X_2), and density (X_3), on two soil shear strength indicators, soil cohesion and internal friction angle, for paddy soils in the plastic state. A prediction model was established to quantify the response of soil cohesion and the internal friction angle to the change in clay content, moisture content, and density.

Our results indicate that all three environmental factors had a significant impact on both soil cohesion and the internal friction angle, and the individual effects of these factors on soil cohesion were in the order of $X_1 > X_2 > X_3$, while the order was $X_2 > X_3 > X_1$ for the internal friction angle. For the interactive factors, the order of contribution to soil cohesion was $X_1X_2 > X_1X_3 > X_2X_3$. The impact of interactive factors on the internal friction angle was in the order $X_1X_2 > X_2X_3 > X_1X_3$; however, none of these factors was significant. Statistical analysis suggested good performance of the model for predicting the soil shear indicators based on soil clay content, moisture content, and density, with R^2 at 0.91 and 0.89 for cohesion and internal friction angle, respectively. After the model setup, our models were successfully validated with another set of soil samples, with all the PBIASs between measured and estimated values within 15% and RRMSEs less than 11%. In conclusion, this study provides a quick and promising prediction of soil shear characteristics for paddy soils in the plastic state, which is a sound basis for the design and improvement of agricultural machinery in paddy fields.

Author Contributions: Conceptualization, Q.J. and Y.W.; methodology, Q.J.; software, M.C. and Z.H.; validation, Q.J., M.C. and J.W.; formal analysis, M.C.; data curation, M.C.; writing—original draft preparation, M.C.; writing—review and editing, Q.J.; visualization, M.C.; supervision, Y.W.; project administration, Y.W.; funding acquisition, Y.W. All authors have read and agreed to the published version of the manuscript.

Funding: This research was funded by the National Key Research and Development Program of China, grant number 2016YFD0700601, and the APC was funded by Zhejiang University.

Institutional Review Board Statement: Not applicable.

Informed Consent Statement: Not applicable.

Data Availability Statement: The data presented in this study are available on request from the corresponding author.

Conflicts of Interest: The authors declare no conflict of interest.

References

1. Yoon, C.G. Wise use of paddy rice fields to partially compensate for the loss of natural wetlands. *Paddy Water Environ.* **2009**, *7*, 357–366. [CrossRef]
2. Kögel-Knabner, I.; Amelung, W.; Cao, Z.; Fiedler, S.; Frenzel, P.; Jahn, R.; Kalbitz, K.; Kölbl, A.; Schloter, M. Biogeochemistry of paddy soils. *Geoderma* **2010**, *157*, 1–14. [CrossRef]

3. Zhang, L.; Zhuang, Q.; He, Y.; Liu, Y.; Yu, D.; Zhao, Q.; Shi, X.; Xing, S.; Wang, G. Toward optimal soil organic carbon sequestration with effects of agricultural management practices and climate change in Tai-Lake paddy soils of China. *Geoderma* **2016**, *275*, 28–39. [CrossRef]
4. Chen, Z.W.; Gu, J.L.; Yang, X.F. A novel rigid wheel for agricultural machinery applicable to paddy field with muddy soil. *J Terramech.* **2020**, *87*, 21–27. [CrossRef]
5. Blanco-Canqui, H.; Lal, R.; Owens, L.B.; Post, W.M.; Izaurralde, R.C. Strength properties and organic carbon of soils in the North Appalachian region. *Soil Sci. Soc. Am. J.* **2005**, *69*, 663–673. [CrossRef]
6. Yang, T. Vehicle Ground Mechanical Shearing Characteristics Research. Master's Thesis, Henan University of Science and Technology, Luoyang, China, 2014.
7. Abubakar, M.S.; Ahmad, D.; Othman, J.; Sulaiman, S. Mechanical properties of paddy soil in relation to high clearance vehicle mobility. *Aust. J. Basic Appl. Sci.* **2010**, *4*, 906–913.
8. Sun, Y. *Agricultural Soil Mechanics*; Agriculture Press: Beijing, China, 1985.
9. Craig, R.F. *Craig's Soil Mechanics*; CRC Press: London, UK, 2004.
10. Amiri, E.; Emami, H.; Mosaddeghi, M.R.; Astaraei, A.R. Shear strength of an unsaturated loam soil as affected by vetiver and polyacrylamide. *Soil Tillage Res.* **2019**, *194*, 104331. [CrossRef]
11. Bekker, M.G. *Introduction to Terrain-Vehicle Systems*; The University of Michigan Press: Ann Arbor, MI, USA, 1969; p. 846.
12. Yang, X. *Geotechnical Test and Principle*; Tongji University Press: Shanghai, China, 2003.
13. Khaboushan, E.A.; Emami, H.; Mosaddeghi, M.R.; Astaraei, A.R. Estimation of unsaturated shear strength parameters using easily-available soil properties. *Soil Tillage Res.* **2018**, *184*, 118–127. [CrossRef]
14. Shen, J.; Yu, Q. Study on the relationship between shear strength and bulk density and moisture content of cohesive soil. *Acta Sin.* **1991**, *2*, 132–138.
15. Liu, L.; Yu, P. Orthogonal analysis for factors influencing clay strength. *J. Chongqing Jiaotong Inst.* **1996**, *15*, 120–124.
16. Xu, J.X. Benggang erosion: The influencing factors. *Catena* **1996**, *27*, 249–263.
17. Zhang, B.; Zhao, Q.G.; Horn, R.; Baumgartl, T. Shear strength of surface soil as affected by soil bulk density and soil water content. *Soil Tillage Res.* **2001**, *59*, 97–106. [CrossRef]
18. Wei, Y.; Wu, X.; Xia, J.; Miller, G.A.; Cai, C.; Guo, Z.; Hassanikhah, A. The effect of water content on the shear strength characteristics of granitic soils in South China. *Soil Tillage Res.* **2019**, *187*, 50–59. [CrossRef]
19. Schjonning, P.; Lamande, M.; Keller, T.; Labouriau, R. Subsoil shear strength—Measurements and prediction models based on readily available soil properties. *Soil Tillage Res.* **2020**, *200*. [CrossRef]
20. Zhang, Y.; Zhong, X.; Lin, J.; Zhao, D.; Jiang, F.; Wang, M.-K.; Ge, H.; Huang, Y. Effects of fractal dimension and water content on the shear strength of red soil in the hilly granitic region of southern China. *Geomorphology* **2020**, *351*. [CrossRef]
21. Yao, Y. Study on the Mechanical Driving Performance of in Soft Soli. Master's Thesis, Nanjing Agricultural University, Nanjing, China, 2009.
22. Liu, D.; Chen, J.; Chen, B. Study on the cone indices and shear strengths of muskeg soils. *Trans. Chin. Soc. Agric. Mach.* **1999**, *30*, 5–8.
23. Zhang, C.; Wang, X.; Zou, X.; Tian, J.; Liu, B.; Li, J.; Kang, L.; Chen, H.; Wu, Y. Estimation of surface shear strength of undisturbed soils in the eastern part of northern China's wind erosion area. *Soil Tillage Res.* **2018**, *178*, 1–10. [CrossRef]
24. Wei, Y.J.; Wu, X.L.; Cai, C.F. Splash erosion of clay-sand mixtures and its relationship with soil physical properties: The effects of particle size distribution on soil structure. *Catena* **2015**, *135*, 254–262. [CrossRef]
25. Ni, Q. Effects of Particle Properties and Boundary Conditions on Soil Shear Behaviour: 3-D Numerical Simulations. Ph.D. Thesis, University of Southampton, Southampton, UK, 2003.
26. Knapen, A.; Poesen, J.; De Baets, S. Seasonal variations in soil erosion resistance during concentrated flow for a loess-derived soil under two contrasting tillage practices. *Soil Tillage Res.* **2007**, *94*, 425–440. [CrossRef]
27. Torri, D.; Santi, E.; Marignani, M.; Rossi, M.; Borselli, L.; Maccherini, S. The recurring cycles of biancana badlands: Erosion, vegetation and human impact. *Catena* **2013**, *106*, 22–30. [CrossRef]
28. Mouazen, A.M. Mechanical behaviour of the upper layers of a sandy loam soil under shear loading. *J. Terramech.* **2002**, *39*, 115–126. [CrossRef]
29. Wuddivira, M.N.; Stone, R.J.; Ekwue, E.I. Influence of cohesive and disruptive forces on strength and erodibility of tropical soils. *Soil Tillage Res.* **2013**, *133*, 40–48. [CrossRef]
30. Rachman, A.; Anderson, S.H.; Gantzer, C.J.; Thompson, A.L. Influence of long-term cropping systems on soil physical properties related to soil erodibility. *Soil Sci. Soc. Am. J.* **2003**, *67*, 637–644. [CrossRef]
31. Horn, R.; Fleige, H. A method for assessing the impact of load on mechanical stability and on physical properties of soils. *Soil Tillage Res.* **2003**, *73*, 89–99. [CrossRef]
32. Johnson, C.E.; Grisso, R.D.; Nichols, T.A.; Bailey, A.C. Shear measurement for agricultural soils—A review. *Trans. Asae* **1987**, *30*, 935–938. [CrossRef]
33. Box, G.E.; Hunter, J.S. Multi-factor experimental designs for exploring response surfaces. *Ann. Math. Stat.* **1957**, *28*, 195–241. [CrossRef]

34. Havaee, S.; Mosaddeghi, M.R.; Ayoubi, S. In situ surface shear strength as affected by soil characteristics and land use in calcareous soils of central Iran. *Geoderma* **2015**, *237*, 137–148. [CrossRef]
35. Fasinmirin, J.T.; Olorunfemi, I.E.; Olakuleyin, F. Strength and hydraulics characteristics variations within a tropical Alfisol in Southwestern Nigeria under different land use management. *Soil Tillage Res.* **2018**, *182*, 45–56. [CrossRef]
36. Luo, D.; Zhuge, Q.; Jiang, C. Rheological properties of paddy field soil and their application. *J. Wuhan Inst. Technol.* **1990**, *2*, 1–9.
37. Fleige, H.; Horn, R.; Stange, F. Soil mechanical parameters derived from the CA database on subsoil compaction. *Adv. GeoEcol.* **2002**, *35*, 359–366.